European Journal of Pharmaceutics and Biopharmaceutics 72 (2009) 509–520

Contents lists available at ScienceDirect

European Journal of Pharmaceutics and Biopharmaceutics

journal homepage: www.elsevier.com/locate/ejpb

Research paper

The use of Eudragit® RS 100/cyclodextrin nanoparticles for the transmucosal administration of glutathione

Angela Lopedota [a], Adriana Trapani [a], Annalisa Cutrignelli [a], Laura Chiarantini [b], Elena Pantucci [b], Rosa Curci [b], Elisabetta Manuali [c], Giuseppe Trapani [a,*]

[a] Dipartimento Farmaco-Chimico, Università degli Studi di Bari, Bari, Italy
[b] Dipartimento di Scienze Biomolecolari, Università degli Studi di Urbino, Urbino, Italy
[c] Istituto Zooprofilattico Sperimentale of Umbria and Marche, Perugia, Italy

ARTICLE INFO

Article history:
Received 19 November 2008
Accepted in revised form 26 February 2009
Available online 10 March 2009

Keywords:
GSH
Eudragit RS 100
Cyclodextrins
Nanoparticles
Transmucosal administration

ABSTRACT

The aim of this work was to develop and characterize new nanoparticle systems based on Eudragit RS 100 and cyclodextrins (CDs) for the transmucosal administration of glutathione (GSH). For this purpose, nanoparticles (NPs) with the mucoadhesive properties of Eudragit RS 100 and the penetration enhancing and peptide protective properties of CDs were prepared and evaluated. The *quasi*-emulsion solvent diffusion technique was used to prepare the NPs with natural and chemically modified (HP-β-CD and Me-β-CD) CDs. The NPs prepared showed homogeneous size distribution, mean diameters between 99 and 156 nm, a positive net charge and spherical morphology. Solid state FT-IR, thermal analysis (DSC), and X-ray diffraction studies suggest that the nanoencapsulation process produces a marked decrease in crystallinity of GSH. The encapsulation efficiency of the peptide was found to be between 14.8% and 24%. The results indicate that mean diameters, surface charges and drug-loaded NPs were not markedly affected by the CD, whereas the presence of the latter influences drug release and to some extent peptide stability and absorption. Finally, it has been shown that CD/Eudragit RS 100 NPs may be used for transmucosal absorption of GSH without any cytotoxicity using the epithelial human HaCaT and murine monocyte macrophage RAW264.7 cell lines.

1. Introduction

Significant advances in biotechnology and molecular biology have led to the discovery of a large number of peptides and proteins potentially useful for the treatment and prevention of disease [1]. However, the use of such compounds in medicine has been limited by their low bioavailability due to the risk of proteolytic degradation and low permeability across biological barriers [2]. Within this context, there is great interest in the development of delivery systems for efficient transport of these drugs to their target tissues along transmucosal routes, including systemic (e.g., oral and nasal) and local (ocular) drug delivery and delivery to immune cells [3,4]. It is known that polymeric nanosystems may enhance the transmucosal transport of drugs having limited penetration abilities whilst preserving their biological activity [4]. In particular, for this purpose nanoparticle systems in which peptides or proteins can be entrapped or embedded have been extensively investigated [5]. Depending on the characteristics of the nanoparticles (NPs) including their size, type of polymer and surface charge, it is possible to enhance the residence time of the drug in contact with the mucosa thus leading to greater efficacy.

The aim of this work was to develop and characterize new nanoparticulate systems based on Eudragit RS 100 and cyclodextrins (CDs) for the transmucosal administration of glutathione (γ-glutamylcysteinylglycine, GSH) as a model peptide drug. The choice of the GSH was motivated by its interesting properties. This peptide is the major non-protein thiol present in significant amounts in living cells. It plays an important role in protection against free radicals and reactive oxygen compounds. Moreover, it is involved in other cellular reactions including the reduction of ribonucleotides, and the regulation of protein and gene expression via thio/disulfide exchange reactions. GSH depletion has also been observed in both lung and neurological disorders such as acute respiratory and Parkinson's diseases [6]. It has also been suggested that GSH may play a role in cancer prevention [7,8]. Furthermore, in HIV-positive patients, systemic GSH and cysteine deficiency has been linked to an increase in virus replication [9]. Interestingly, it has been shown that abnormal levels of GSH occur in ocular diseases such as retinal damage [10], glaucoma, and

* Corresponding author. Dipartimento Farmaco-Chimico, Facoltà di Farmacia, Università degli Studi di Bari, Via Orabona 4, 70125 Bari, Italy. Tel.: +39 080 5442764; fax: +39 0805442754.
E-mail address: trapani@farmchim.uniba.it (G. Trapani).

0939-6411/$ - see front matter © 2009 Elsevier B.V. All rights reserved.
doi:10.1016/j.ejpb.2009.02.013

age-related macular degeneration. In addition, the inhibitory effect of GSH on oral enzymatic degradation of therapeutic peptides has also been shown [11].

Eudragit RS 100 [i.e., poly(ethyl acrylate, methyl-methacrylate, and chlorotrimethyl-ammoniumethylmethacrylate) co-polymer containing quaternary ammonium groups in 4.5–6.8%] was selected because of its well-established mucoadhesive characteristics. This polycation is insoluble at physiological pH but swells in water [12]. Moreover, this mucoadhesive, non-biodegradable positively charged polymer has been used for developing NPs for the ophthalmic and oral administration of ibuprofen [12] and cyclosporins [13], as well as nano- and micro-fibres used as scaffolds in tissue engineering [14].

Recently, it has been shown that the incorporation of cyclodextrins (CDs) into polymeric NPs can increase the drug loading and modify drug release [15]. It is now accepted that the incorporation of drug/CD mixtures or complexes into polymeric matrices can improve hydration of the matrix and modify drug solubility and diffusivity, leading to modified drug release from the polymeric system. On the other hand, CDs are able to interact with the hydrophobic side chains of peptide or protein compounds preventing, to some extent, their degradation [16,17]. Furthermore, CDs may reduce the intrinsic resistance of the physiological barriers due to their well-established penetration enhancing properties [18].

Like other peptides, GSH can suffer both chemical and enzymatic hydrolysis leading to the corresponding free amino acids. The thiol group of GSH can be oxidized both enzymatically and non-enzymatically to the corresponding glutathione disulfide (GSSG), which is a devoid of radical scavenging activity [19]. Nanoencapsulation of GSH in an Eudragit RS 100 polymeric system containing CDs may protect the peptide against chemical and/or enzymatic degradation.

Based on these considerations, it seemed of interest to combine in a single nanocarrier system the mucoadhesive properties of Eudragit RS 100 with the penetration enhancing and peptide protective properties of CDs in order to achieve transmucosal drug delivery. A specific advantage of using a non-biodegradable polymer is the absence of problems associated with degradation products of the macromolecule. It should be noted that we already reported on GSH/CDs-loaded Eudragit RS 100 microparticles [20,21] but, to the best of our knowledge, only one study has been reported by Couvreur and coworkers on GSH nanoencapsulation where a biodegradable, non-mucoadhesive and neutral polymer, i.e., poly(isobutylcyanoacrylate) (PiBCA), was employed [22].

In the present study, NPs were prepared using GSH and Eudragit RS 100 alone or in the presence of CDs. Natural α, β and γ) and chemically modified hydroxypropyl- (HP-β-CD) and methyl- (Me-β-CD) β-CDs were used. The physicochemical properties, drug release kinetics, stability of GSH-containing NPs towards enzymatic attack by γ-glutamyltranspeptidase were investigated. Moreover, the cytotoxicity of NPs *in vitro* was studied on human epithelial and murine monocyte macrophage cell lines along with transport studies through frog intestine.

2. Materials and methods

2.1. Materials

Reduced GSH, glutathione disulfide (GSSG), perchloric acid (70%), γ-glutamyltranspeptidase (from equine kidney Type VI, 11 U/mg), and Dulbecco's modified Eagle's medium (DMEM) were purchased from Sigma–Aldrich (Milan, Italy). Polyvinylalcohol (PVA, polymerization degree 500 (viscosity of a 4% aqueous solution at 20 °C: 5 mPa s)) was supplied by Fluka. Eudragit RS 100 (Röhm GmbH & Co.) was kindly donated by Rofarma (Gaggiano, Milan, Italy). Acetone (RP grade), Acetonitrile (HPLC grade), was purchased from Baker (Deventer, Holland). 2-Hydroxypropyl-β-cyclodextrin (HP-β-CD) with a degree of substitution of 5.88 (from ^{1}H-NMR data) was donated by Roquette (Cassano Spinola, Italy). α-, β-, γ-CD and mono methyl-β-cyclodextrin (Me-β-CD) were gifts from Waker-Chemie (Peschiera Borromeo, Italy).

2.2. Quantitative analysis of GSH

HPLC analysis. High-performance liquid chromatography (HPLC) analyses were performed with a Waters (Waters Corp., Milford, MA) instrument equipped with a Model 600 pump and photodiode array detector 2996 (set at 220 nm), an autosampler (717 plus), and Empower software. For analysis, 20 μl of sample was injected onto a reversed phase Synergy Hydro-RP (25 cm × 4.6 mm; 4 μm particles; Phenomenex, Torrance, CA) column with a precolumn C18 insert and eluted with 1:99 (v:v) acetonitrile: 0.025 M phosphate buffer (pH 2.7) isocratically. A flow rate of 0.7 ml/min was maintained and the column effluent was monitored continuously at 220 nm. Quantification of the compounds was carried out by measuring the peak areas compared to standards chromatographed under the same conditions. Standard calibration curves were prepared at 220 nm wavelength using 0.025 M phosphate buffer (pH 2.7) as solvent and were linear ($r^2 > 0.999$) over the range of tested concentrations (6.51×10^{-6} to 3.25×10^{-3} M). The retention times of GSH and GSSG were 7.2 and 18 min, respectively. Under these conditions, the quantification limit (LOQ), defined as the analyte concentration which could be analyzed with acceptable precision and accuracy, was found to be 2 μg/ml for both GSH and GSSG. The linear range for this assay was confirmed over the range 2–1000 μg/ml.

2.3. Preparation of GSH/CD complexes in aqueous solutions

GSH/CD complexes were prepared with GSH (0.52 mmol) and an equimolar amount of CD in 10 ml of deionized water (26 ml of deionized water for β−CD) with a magnetic stirring for 24 h at room temperature and under nitrogen atmosphere. The mixture was then filtered (0.45 μm) and the amount of GSH in the filtered solution determined.

2.4. Preparation of GSH-loaded Eudragit RS 100 nanoparticles

NPs were prepared using the *quasi*-emulsion solvent diffusion technique (QSESD) previously reported [12,23]. Eudragit RS 100 (280 mg) was dissolved in acetone (3 ml) at room temperature and this organic phase was poured into an aqueous phase consisting of a solution of GSH (45 mg in 5 ml of deionized water) and 10 ml of an aqueous solution of PVA 0.4% w/v (final pH 3). The resulting mixture was homogenized using a T25 Ultraturrax homogenizer (Janke and Kunkel, Germany) equipped with an S25N dispersing tool at 13,000 rpm for 7 min. Removal of traces of acetone was carried out under reduced pressure at 28 °C with a rotavapor (Büchi) apparatus. The suspension was then transferred into Eppendorf vials and centrifuged at 13,200 rpm for 60 min (Eppendorf centrifuge, model 5415 D). The NPs thus obtained were finally resuspended in 1 ml of water and lyophilized for 24 h at −50 °C (Cinquepascal, Lio 5P model freeze-drier, Milan, Italy). These formulations were stored at 4 °C until further use.

The above-mentioned procedure was also followed to prepare a further formulation containing as aqueous phase a solution of GSH (45 mg in 5 ml of borate buffer) added to 5 ml of borate buffer 0.06 M and 10 ml of a solution of PVA 0.4% w/v in borate buffer 0.06 M (final pH 7.8).

2.5. Preparation of GSH/CD complexes-loaded Eudragit RS 100 nanoparticles

NPs containing GSH/CD complexes were prepared following the procedure in Section 2.4 with a little modification. The appropriate volume of the solution containing the GSH/CD complex (Section 2.3) equivalent to 45 mg of GSH was added to an aqueous solution of PVA 0.4% w/v. To this mixture, an organic phase consisting of acetone (3 ml) and Eudragit RS 100 (280 mg) was added as already described. Working-up as above, the required NPs containing the GSH/CD complexes were obtained.

2.6. Physicochemical characterization of the nanoparticles

The mean size and polydispersity index (P.I.) of the NPs suspension were measured using a Zetasizer Nano ZS (Malvern Instruments Ltd., Worcestershire, UK) after suitable dilution of bulk suspensions in demineralized water. The P.I. values range from 0 to 1; a higher value indicates a less homogeneous NP size distribution. The zeta potentials were determined by laser Doppler velocimetry with the same instrument. All samples were diluted 1:20 with a 1 mM KCl solution to maintain constant ionic strength and an adequate concentration of particles. These dispersions were examined with the Zetasizer apparatus. Three measurements were made on at least six different batches of each NP formulation to determine the mean particle diameter and zeta potential together with the corresponding standard deviation.

The residual PVA content was determined using a reported method [24], based on the formation of a stable complex of PVA–iodine in the presence of boric acid. Briefly, 5 mg of lyophilized NPs was treated with 0.1 N NaOH (2 ml). To the mixture 0.5 N HCl (0.9 ml) was added and the suspension diluted to 5 ml with water was centrifuged at 13,200 rpm for 15 min. Two milliliters of supernatant were treated with 1.2 ml of boric acid solution (4.0% w/v) and 0.2 ml of iodine solution (1.27% iodine and 2.5% potassium iodide in distilled water w/v), adjusting the volume to 4 ml with water. The percentage of residual PVA was calculated by measuring the absorbance at 644 nm (Perkin Elmer Lamba Bio 20 spectrophotometer).

The morphological examination of Eudragit RS 100 NPs was performed by transmission electron microscopy (TEM) (CM12 Philips, Eindhoven, The Netherlands). Drops of water-resuspended NPs were stained with 2% (w/v) phosphotungstic acid and were placed on copper grids with Formvar® films for TEM observation.

2.7. Solid state characterization of the nanoparticle systems

2.7.1. Fourier transform infrared spectroscopy

Fourier transform IR spectra were obtained on a Perkin Elmer 1600 FT-IR spectrometer. Samples were prepared in KBr disks (2 mg sample in 200 mg KBr). The samples were scanned from 450 to 4000 cm^{-1} with a resolution of 1 cm^{-1}. Eight scans were performed for each IR spectrum.

2.7.2. Thermal analysis

DSC curves were obtained with a Mettler Toledo DSC 822e Star^e 202 System equipped with an automatic thermal analysis program. Aliquots of about 5 mg of each sample were placed in an aluminium pan without pin. Conventional DSC measurements were performed by heating the sample to 250 °C at a rate of 5 °C/min under a nitrogen flow of 20 cm^3/min. Indium (purity 99.9%) was used as the standard for calibrating temperature. Reproducibility was checked by running the sample in triplicate.

2.7.3. X-ray diffractometry

X-ray diffraction (XRD) patterns were recorded on a Philips X'PERT PRO X-ray diffractometer using Cu Kα radiation, a voltage of 40 kV, a current of 40 mA, and a scanning rate of 0.5 °/min.

2.8. Determination of cyclodextrin content within the nanoparticles

The CD content within the NPs was quantified by spectrophotometric analysis of the fading of phenolphthalein alkaline solutions in the presence of the examined cyclodextrin [25]. Briefly, a 3 mM phenolphthalein stock solution in methanol was diluted 1:100 in 0.05 M carbonate buffer (pH 10.5). Freeze-dried NPs (obtained by freeze-drying 1 ml of NP suspension) were dissolved in 500 μl of acetone and, after 30 min, 1000 μl of water was added. Four hundred microliters of this mixture were added to 2.6 ml of diluted phenolphthalein solution prepared as described above and were centrifuged at 13,200 rpm for 10 min. The absorbance at 553 nm of the resulting solution was measured with a Perkin Elmer Lamba Bio 20 spectrophotometer. The CD content was calculated by comparing the results with those of a standard curve obtained using standard CD solutions. Linearity was checked from 0.0125 mg/ml to 0.2 mg/ml (from 0.250 mg/ml to 4.05 mg/ml for Me-β-CD).

2.9. Determination of GSH encapsulation efficiency

The amount of GSH embedded in the NPs was calculated from the difference between the total amount incorporated in the NP formation medium and the amount of non-embedded GSH remaining in the aqueous suspending medium. The latter amount was determined following the separation of GSH-loaded NPs from the aqueous suspension medium by centrifugation at 13,200 rpm for 60 min. GSH was determined by HPLC as described above. Results are expressed as encapsulation efficiency (E.E.) calculated as actual drug loading/theoretical drug loading × 100. Three measurements were made on at least six different batches of each NP formulation.

2.10. Interaction of nanoparticles with mucin

Ten milligrams of porcine mucin (Type II, Sigma, Milan, Italy) were dispersed in PBS pH 6.8 (10 ml) and the mixture was maintained at 37 °C for 24 h under shaking (150 rpm). Then, appropriate amounts of GSH-containing NPs without CDs or NPs without GSH and CD were dispersed in the mucin mixture (mucin/polymer weight ratio equal to 0.1) and were incubated at 37 °C under shaking (150 rpm) for 1, 2, 4, 6, 15 h. After each incubation time, the transmittance of the samples was recorded at 500 nm wavelength. Carbopol 934, polyacrylic acid and PEG 6000 (mucin/polymer weight ratio equal to 1) were used as control.

2.11. In vitro release studies

In vitro release profiles of GSH from NPs with or without CDs were examined in two different media, namely HCl pH 1.2 (0.063 M) and phosphate buffer pH 6.8 (0.05 M). An appropriate amount of NPs containing about 3 mg of the GSH was suspended in buffer solution (6 ml) and vortexed to achieve a homogenous suspension. The latter was then placed in a screw-capped test tube and maintained at 37 °C in a shaking bath (150/min, ISCO, Milan, Italy). At scheduled time intervals, samples (300 μl) were withdrawn, centrifuged (13,200 rpm for 5 min) and the supernatant was removed. Volumes of dissolution medium equal to that withdrawn were immediately added. The GSH content of the removed supernatant was determined by HPLC. All experiments were carried out in triplicate. Standard deviation of measurements < 10%.

2.12. Assessment of NP stability to enzymatic degradation

Non-encapsulated GSH and GSH/Me-β-CD-loaded Eudragit RS 100 NPs were used as representative formulations for stability studies.

γ-Glutamyltranspeptidase. The γ-glutamyltranspeptidase solution was prepared by dissolving 1.2 mg of γ-glutamyltranspeptidase in distilled water (2 ml) and then, 0.8 ml of this solution was mixed with 5.2 ml of phosphate buffer pH 6.8.

Pure GSH (3.8 mg) was solubilized in the γ-glutamyltranspeptidase solution prepared as above in a screw-capped test tube and was incubated at 37 °C in a shaking (100 rpm) and thermostatically controlled water bath. At given time intervals, aliquots of 400 μl were withdrawn, and the enzymatic reaction was stopped by addition of 10% perchloric acid (250 μl). Each sample was centrifuged at 13,200 rpm for 15 min and the supernatant was diluted 1:1 with 0.025 M phosphate buffer pH 2.7 and the remaining intact peptide was determined by HPLC. The stability kinetics were followed for up to 4 h.

Pure GSH (3.8 mg) and an appropriate amount of GSH/Me-β-CD-loaded NPs equivalent to 3.8 mg of GSH were suspended in the γ-glutamyltranspeptidase solution prepared as above in a screw-capped tube and were incubated at 37 °C in a shaking (150 rpm) and thermostatically controlled water bath. By working up as above the GSH stability in the presence of γ-glutamyltranspeptidase was determined. All experiments were performed in triplicate and $t_{1/2}$ was measured by the disappearance of GSH. Standard deviation of measurements ± 10%.

2.13. Cell culture and MTS assay in HaCaT and RAW 264.7 cells

Human epithelial cell line (HaCaT) and murine monocyte macrophage cell line (RAW 264.7) were cultured in DMEM supplemented with 10% heat-inactivated foetal calf serum (FCS), 2.0 mM glutamine and 1% antibiotic. Cells were maintained in exponential growth at 37 °C in a humidified atmosphere of 95% air–5% CO_2.

2.14. Cellular toxicity

The Promega CellTiter 96® Aqueous Non-Radioactive Cell Proliferation Assay (Promega) was used to measure the cytotoxicity of both control Eudragit RS 100 NPs and Me-β-CD-loaded Eudragit RS 100 NPs with or without GSH by determining the number of viable HaCaT and RAW 264.7 cells in culture. HaCaT and RAW 264.7 cells were seeded in 96-well plates (Greiner, International PBI, Italy) at 0.4×10^5 cells/ml and 0.7×10^5 (100 μl/well) respectively, and treated with several concentrations 0–500 μg/ml for 24, 48 and 72 h.

The MTS (3-(4,5-dimethylthiazol-2-yl)-5-(3-carboxymethoxyphenyl)-2-(4-sulfopnenyl)-2H-tetrazolium) assay is based on the ability of viable cells to convert a soluble tetrazolium salt to a formazan product. After exposure, the MTS/PMS reagent was added and cell cultures were incubated at 37 °C for 4 h. At the end of incubation period, absorbance was recorded on a Microplate Reader (Benchmark, Bio-Rad) at 492 nm and at a reference wavelength of 630 nm. The experiments were run in hextuplicate for three different experiments. The results are expressed as percentage of control.

2.15. Evaluation of cellular morphology by light and electron microscopy analysis

For light microscopy HaCaT cells were seeded at 6×10^4/ml onto cover slides placed into a six-well plate and untreated or treated (Eudragit RS 100 NPs, GSH-Eudragit RS100 NPs) for 24, 48 h. At the end of incubation period the medium was removed from each well and thoroughly washed with phosphate buffer solution (PBS), air-fixed, stained with May Grünwald Giemsa and examined at 1000× magnification with a Leica DMR Fluo HC microscope.

For Transmission Electron Microscopy (TEM) the HaCaT cells were fixed in 2.5% glutaraldehyde (TAAB, England) in 0.1 M phosphate buffer (v/v), pH 7.4 for 2 h at 4 °C and post-fixed in 1% osmium tetroxide (OsO_4) (Next Chimica, South Africa) in 0.1 M phosphate buffer (v/v) for 1 h at 4 °C. The samples were then dehydrated in a graded series of ethanol, incubated in propylene oxide (TAAB, England) for 10 min at room temperature and embedded in Epon 812. The resin blocks were solidified at 60 °C for 24 h. Semithin sections were stained with 1% blue toluidine (w/v) pH 3.5. Silver colour ultra-thin sections were collected onto copper grids coated with a Formovar® layer and double stained with uranyl acetate-lead citrate. Samples were examined and photographed at 80 kV on a CM12 STEM electron microscope (Philips, Eindhoven, The Netherlands).

2.16. Determination of mitochondrial membrane potential ($\Delta\Psi$)

Cells were incubated with or without 0–250 μg/ml of Eudragit RS 100 NPs and Me-β-CD-loaded Eudragit RS 100 NPs with or without GSH. After 0, 12, 24 and 48 h an aliquot of cells was stained with 2 μmol of 5,5′,6,6′-tetrachloro-1,1′,3′,3′-tetraethylbenzimidazolylcarbocyanine iodide (JC-1) (Molecular Probe) for 20 min at 37 °C in 5% CO_2. At the end of the incubation period, the cells were washed twice in cold PBS and resuspended in a final volume of 500 μl. The samples were analyzed using a FACScan flow cytometer and CellQuest software (Becton Dickinson, San Jose, CA, USA).

2.17. Transport studies by using frog intestinal sacs

In intestinal sac experiments, animal care and handling throughout the experimental procedure were in accordance with the European Community Council Directive of 24 November 1986 (86/609/EEC). Healthy frogs of the species *Rana esculenta*, a European frog (Animali da Laboratorio R. Orefice Arzano Napoli) were housed in a cold room, in an aquarium without food. The aquarium was thoroughly washed once a week. The frogs were killed by decapitation and pithing of the spinal cord, and small intestines were quickly removed by laparotomy, a midline abdominal incision. The excised piece of intestine was immediately washed with Frog Ringer (FR) solution at room temperature to remove the intestinal content. The FR solution had the following composition: NaCl 112 mmol, KCl 5.0 mmol, $CaCl_2$ 1.0 mmol, $NaHCO_3$ 2.5 mmol, pH 6.0. The osmolalities were measured for 100 μl samples using the Micro-Osmometer Automatic Type 13 RS (Hermann Roebling Messtechnik, Berlin, Germany) and were found to be 228 ± 2.8 mOsm/Kg.

Intestinal segments of approximately 5 cm in length (starting immediately below the stomach) were tied at one end with a silk suture. The integrity of these intestinal membranes was checked by using phloridzin as internal standard at the concentration of 160×10^{-6} M. The sacs were filled with a FR solution of GSH or a mixture of an aqueous solution of GSH and resuspended NPs at 50% (v/v) and the volume of the donor compartment was in the range 0.1–0.3 ml. The sacs were sealed, and immersed in a vial (2.70 cm width × 5.73 cm high) containing a volume of FR in the range of 1.0–2.0 ml and the vials were put on a water shaking bath (Isco mod. SBH Milan, Italy) set at 26 ± 0.1 °C with a speed of 100 agitations per min for 6 h of incubation. Thus, at prefixed time withdrawals, the amount of GSH permeated was determined by HPLC and the initial volume of release medium was maintained by refilling with fresh FR.

2.18. Statistical analysis

The statistical analysis for the determination of differences in the measured properties between groups was accomplished using one-way analysis of variance (ANOVA) followed by the Tukey post hoc tests (GraphPad Prism version 4 for Windows, GraphPad Software, San Diego, CA). Differences were considered statistically significant at $p < 0.05$.

3. Results and discussion

The main objective of the present study was to prepare and characterize new nanoparticle systems which combine the mucoadhesive properties of Eudragit RS 100 with the penetration enhancing and peptide protective properties of CDs, evaluating their potential for transmucosal delivery of GSH, selected as a model peptide drug.

First of all, we gained information on the possible interaction between GSH and CDs. In this regard, it should be noted that evidence of GSH inclusion into α- and HP-β-CD was already obtained by NMR spectroscopic studies [26,20]. Similar investigations were preliminarily carried out with the remaining CDs herein considered. In particular, the proton chemical shift differences of GSH protons due to the addition of β, γ and Me-β-CD in equimolar amount were detected. It was found that the GSH proton chemical shifts changed in the presence of β-, γ-, and Me-β-CD and moreover these variations are more consistent for protons of the glutamyl moiety (data not shown). These results suggest that also in these cases a weak interaction between GSH and CDs occurs. The peptide backbone could be partially included in the cavity of CD while the polar carboxylic acid and amine groups and thiol moiety remain outside the cavity.

3.1. Characterization of nanoparticle systems

3.1.1. Nanoparticle size, zeta potential and morphology

As mentioned above, GSH-loaded NPs were prepared by the QSESD technique. The NPs prepared were characterized for particle size and zeta potential and the results are shown in Table 1. As can be seen, the mean diameter of GSH-containing NPs without CDs was found to be 115 nm, while those with CDs were in the range of 99–156 nm. The smallest NPs (i.e., 99 nm) were those containing β-CD while the largest were those with Me-β-CD. The NPs prepared without GSH and CDs, used as control, had a mean diameter of 123 nm. However, it should be noted that there were no significant differences in mean diameter between the control NPs and those containing GSH without CDs. In all cases the Polydispersity index (P.I.) fell within the range 0.21–0.35. As known, the P.I. is a parameter used to define the particle size distribution of NPs, it is a dimensionless number and ranges from a value of 0.01 for monodispersed particles up to values of around 0.5–0.7. Values greater than 0.7 are characteristic of samples with a very broad size distribution [27]. Therefore, it can be stated that the Eudragit RS 100 based NPs prepared by the QSESD technique were characterized by a homogeneous size distribution. The net charge on the NPs was positive and between +40.5 mV and +48.8 mV for the control NPs and those prepared with HP-β-CD, respectively. Again, no significant difference in zeta potential was found between the control NPs and those containing GSH, prepared in both the presence and absence of CDs. From these results it can be concluded that both the mean diameter and the surface charge on NPs were not markedly affected by the presence of CDs and/or GSH.

Table 1
Size, zeta potential, yield and encapsulation efficiency of GSH- and GSH/CD-loaded Eudragit RS 100 nanoparticles.

NP formulation	Size (nm)	P.I.	Zeta potential (mV)	Encapsulation efficiency (%)	PVA content[a] (w/w) (%)
Without GSH and CD	123 ± 9	0.22 ± 0.010	+ 40.5 ± 1.8	–	0.4 ± 0.1
GSH	115 ± 8	0.21 ± 0.015	+ 43.4 ± 3	14.8 ± 5.2	0.6 ± 0.02
GSH/α-CD	137 ± 48	0.25 ± 0.047	+ 43.9 ± 3.6	17.5 ± 6.5	0.9 ± 0.1
GSH/β-CD	99 ± 34	0.26 ± 0.050	+ 44 ± 3.6	16.2 ± 7.4	12.5 ± 1.6
GSH/γ-CD	140 ± 14	0.24 ± 0.014	+ 41.1 ± 4.7	22.8 ± 6.4	2.5 ± 0.1
GSH/HP-β-CD	142 ± 23	0.28 ± 0.052	+ 48.8 ± 1.6	18.6 ± 4.5	2.5 ± 0.1
GSH/Me-β-CD	156 ± 40	0.35 ± 0.060	+ 44.2 ± 4.1	23.9 ± 6.3	1.9 ± 0.2

[a] Weight (mg) of PVA per 100 mg of nanoparticles.

The presence of residual PVA on NPs was confirmed using a well-known method [24]. As shown in Table 1, except for β-CD, the percentages of PVA detected were low and this may be due to the low PVA concentration used in the manufacturing method [24]. However, a clear trend was observed with the CD-containing NPs showing higher residual PVA concentrations than the control with or without GSH. The rank order observed for the residual PVA content on the CD-containing NPs (i.e., β-CD >>> γ-CD = HP-β-CD > Me-β-CD) parallels the specific surface area of the corresponding NPs and this is not surprisingly since it is well known that particles with large specific surface areas are good adsorbents. Thus, the higher residual PVA associated with the β-CD could be related to the smaller size of the corresponding NPs and consequently to their higher specific surface area. In contrast, the lower residual PVA content observed with Me-β-CD-containing NPs could be related to their lower specific surface area. γ-CD- and HP-β-CD-NPs showed the same residual PVA content since they possess the same mean diameter.

A spherical shape of the NPs was observed by TEM, irrespective of the sample (i.e., control-, GSH-, and GSH/CD-containing NPs) as shown in Fig. 1. In general, the hydrodynamic diameter of the particles measured by light scattering has been found to be larger than the size estimated by TEM where the high-vacuum drying of the sample suspension will tend to reduce the particle size. Here, the TEM results gave diameters comparable to those obtained by light scattering, which is presumably due to modest swelling of the polymer under the experimental conditions used.

3.2. Solid state characterization of the nanoparticles

To assess whether interactions between GSH and the Eudragit RS 100 polymer occur and whether the GSH was incorporated into the NPs in its crystalline or amorphous form, FT-IR, powdered X-ray diffraction, and DSC analyses were used. FT-IR spectra of pure GSH and of all the GSH-loaded NPs were recorded (Fig. 2). The spectrum of pure GSH showed strong absorption bands assigned to carbonyl- and amide-stretching (1713 cm^{-1} and 1600 cm^{-1}, respectively), as well as the absorption band of the —SH group at 2525 cm^{-1}. IR spectra of the NPs were essentially similar to those of the pure polymer. They are characterized by a broad band at 1734 cm^{-1} due to the carbonyl group of the polyester. In addition, a weak band between 1640 and 1650 cm^{-1} assigned to the corresponding CD was also present. Moreover, no absorption band due to the thiol group at 2525 cm^{-1} was detected in the FT-IR spectra of NPs, and it can be related to the low peptide encapsulation efficiency (see Section 3.4). The disappearance of the absorption band at 2525 cm^{-1} did not allow us to gain information about possible interactions between GSH and the polymer in the solid state. Fig. 2 shows the X-ray diffraction patterns of pure GSH and CD-containing NPs. The X-ray diffraction spectrum of crystalline GSH was characterized by one intense peak at 2ϑ 22.3° and two peaks

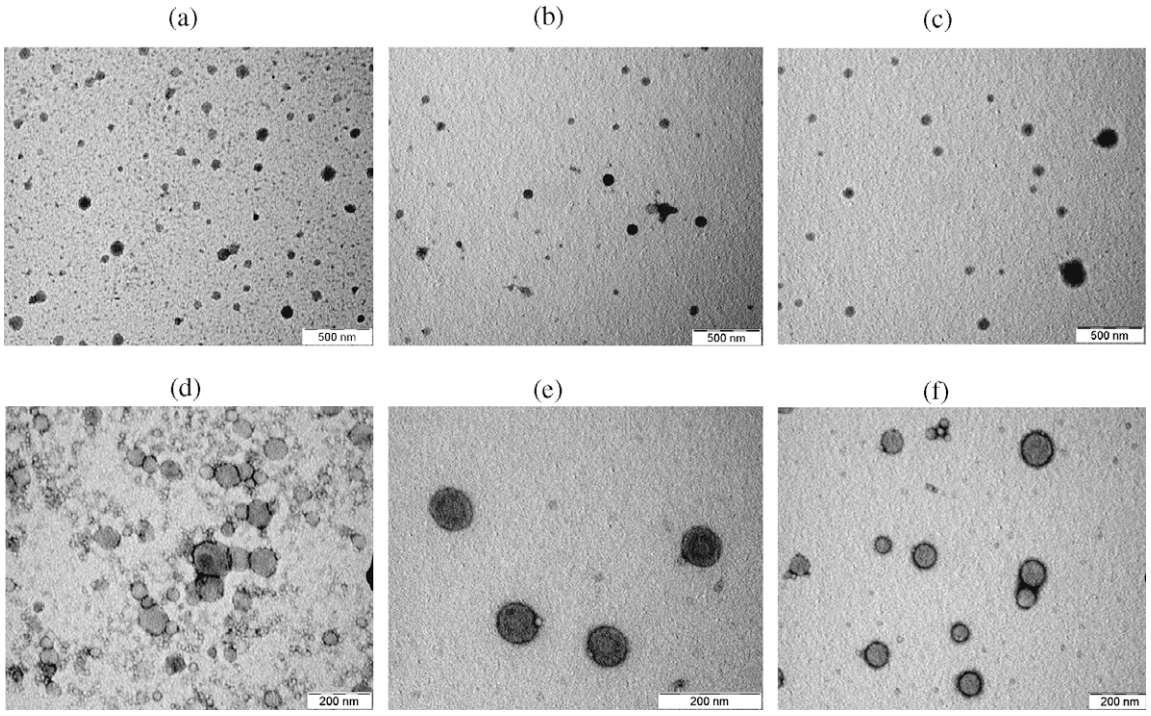

Fig. 1. TEM micrographs of NPs (a) without GSH or CD; (b) NPs loaded with GSH alone; (c) NPs loaded with GSH/Me-β-CD at lower magnification (500 nm bar); (d) Without GSH or CD; (e) NPs loaded with GSH alone; (f) NPs loaded with GSH/Me-β-CD at higher magnification (200 nm bar).

of low intensity at 2ϑ 9–11°. In the X-ray spectra of the NPs these peaks were either absent or strongly reduced and a halo pattern resulted. DSC profiles of all the formulations were carried out together with those of pure GSH showing a single endothermic peak at 196 °C corresponding to melting of the drug (Fig. 2). In the DSC profiles of all the loaded NPs the peak at 196 °C is not present and the thermograms are essentially similar to that of the Eudragit RS 100 polymer. These results, taken together, suggest that the nano-encapsulation process produces a marked decrease in crystallinity of GSH and/or confers to this drug a nearly amorphous state.

3.3. Cyclodextrin content of nanoparticles

The NPs were analyzed in order to evaluate their CD content. The observed presence of residual PVA on NPs did not allow the use of elemental analysis for CD content determination and an alternative approach was necessary. The CD content was successfully determined by spectrophotometric analysis based on the fading of phenolphthalein alkaline solutions in the presence of the CD on NPs both with and without GSH. However, it was found that the assay did not work well with all the CDs studied [25]. Thus, in the case of α-CD no fading of phenolphthalein was observed. The failure to determine α-CD content using this spectrophotometric assay has already been noted [25]. Table 2 shows the results obtained. As can be seen, except for γ-CD, the CD content observed for NPs without GSH were slightly greater than those with the tripeptide. Furthermore, the highest residual CD percentages were found with Me-β-CD and γ-CD (7.8% and 6%, respectively) GSH-loaded NPs. This finding may be accounted for assuming both that the complexes GSH/γ-CD and GSH/Me-β-CD are the most stable ones and that the GSH is better encapsulated in NPs as CD complex. If so, it is not surprising to observe that the highest CD content values correspond just to NPs prepared in the presence of Me-β-CD and γ-CD since in these cases the highest drug GSH encapsulation efficiencies (E.E.s) were observed (Table 1).

3.4. Drug loading

Table 1 also reports the GSH E.E.s of the prepared NPs whose values were in the range of 15–24%. Although the E.E.s are quite relatively low, it should be noted that they are essentially comparable with those observed by using PiBCA-based NPs [22]. However, in the case of Eudragit RS 100 NPs, GSH starting concentrations up to 3 mg/ml are well tolerated unlike that observed with PiBCA. In fact, it is reported that for GSH starting concentrations higher than 1 mg/ml, aggregates but not PiBCA NPs were formed [22]. It seems from the reported data in Table 1 that, although the differences are not statistically significant, the type of CD employed does slightly affect the GSH E.E. In fact, a clear trend was observed, with NPs containing more water-soluble CDs (Me-β-CD, γ-CD and HP-β-CD) being characterized by a slightly increased E.E. However, together with the water solubility of CDs, other factors should be involved to account for the rank order in drug loading observed. In fact, the E.E. of the highly water soluble HP-β-CD containing NPs resulted comparable with that of the less water-soluble CD, i.e., the β-CD. It may be hypothesized that also the steric hindrance of the substituent of the chemically modified CD plays an important role in this regard. Assuming as above proposed that the GSH is better encapsulated in NPs as CD complex and being the size of the hydroxypropyl group greater than the methyl one, it may be possible that complexation with Me-β-CD is more efficient than with HP-β-CD. In an attempt to increase the E.E. values, NPs were also prepared in 0.06 M borate buffer at pH 7.8 without CDs taking into account that GSH (isoelectric point, pI, 5.77) is positively charged at pH 3, but negatively at pH 7.8. Consequently, it seemed reasonable to evaluate whether electrostatic interactions between the negatively charged GSH and the Eudragit RS 100 ammonium groups may play a role in the binding of GSH to the polycation-containing NPs. It was found that NPs prepared in borate buffer exhibited a bimodal size distribution. In fact, they showed a mean diameter of 218 ± 53 nm and they were obtained together with particles of 1181 ± 359 nm in diameter and P.I.

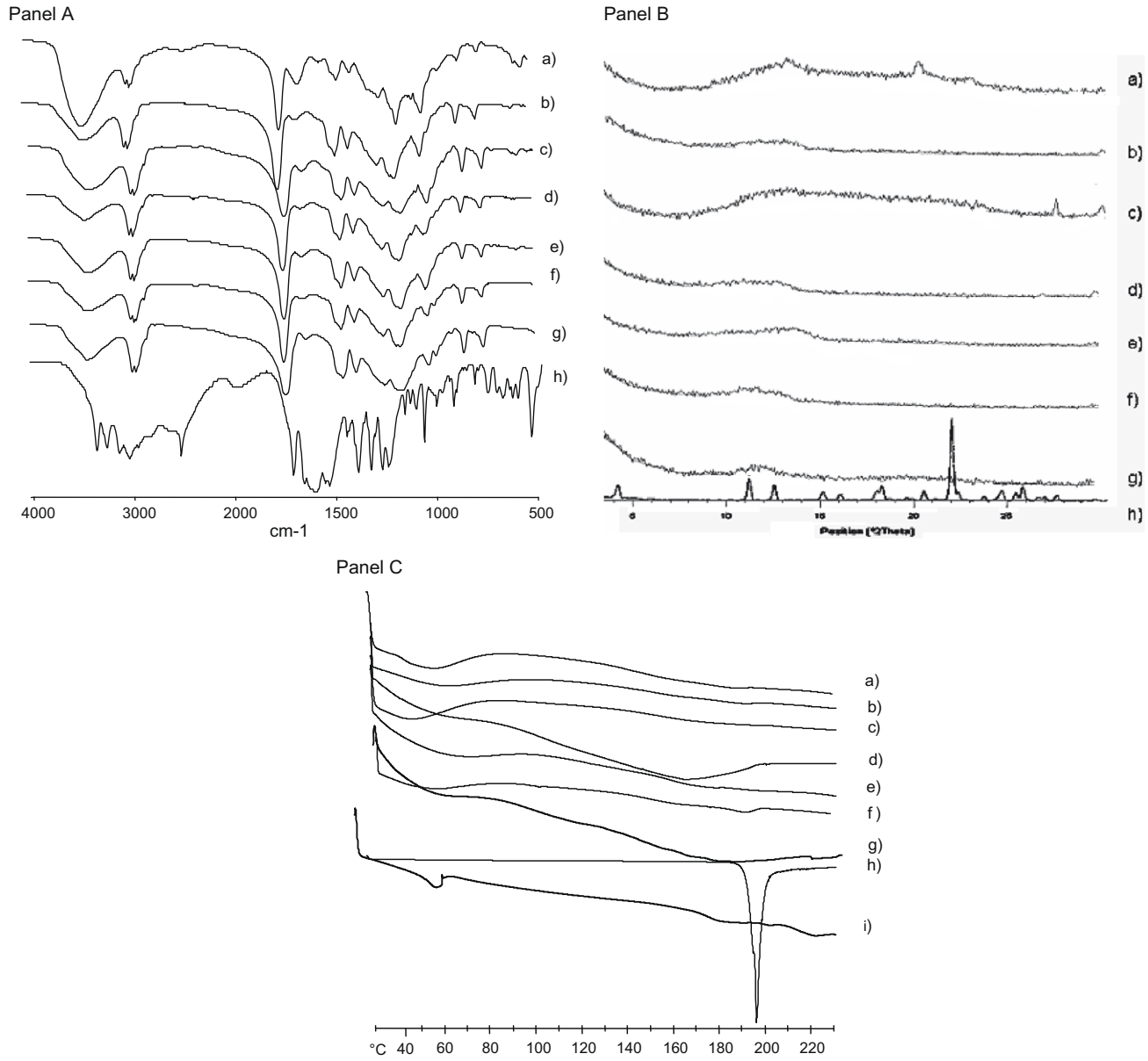

Fig. 2. FT IR (A) and PXRD (B) spectra of NPs with: (a) GSH/α-CD, (b) GSH/β-CD, (c) GSH/γ-CD, (d) Me-β-CD, (e) HP-β-CD, (f) without GSH or CD, (g) GSH. FT-IR and PXRD spectra of (h) pure GSH. In (C) DSC profiles of NPs with (a) GSH/α-CD, (b) GSH/β-CD, (c) GSH/γ-CD, (d) Me-β-CD, (e) HP-β-CD, (f) without GSH or CD, (g) GSH. DSC profiles of (h) pure GSH; (i) pure Eudragit RS 100 are shown.

0.70 ± 0.10 which is indicative of a very broad size distribution. The net charge on the NPs prepared in alkaline medium was found to be less positive and significantly different from those obtained at low pH (+18 ± 3 mV). The GSH E.E. of the NPs prepared in alkaline medium was 18.6 ± 8.0 which is essentially similar to the control formulation prepared in acidic medium. From these results it can be concluded that the role played by electrostatic interactions in the association of GSH should not be relevant and other forces such as hydrogen bonding interactions may account for the encapsulation of the GSH into the NPs as well.

Table 2
Cyclodextrin content of selected CD-containing nanoparticles.[a]

NP formulation containing GSH	CD content[b] (%)	NP formulation without GSH	CD content[b] (%)
GSH/α-CD	ND	α-CD	ND
GSH/β-CD	2.7 ± 1.2	β-CD	4.5 ± 0.8
GSH/γ-CD	6.0 ± 0.3	γ-CD	4.0 ± 1.4
GSH/HP-β-CD	2.5 ± 0.1	HP-β-CD	3.5 ± 0.6
GSH/Me-β-CD	7.8 ± 0.5	Me-β-CD	11.6 ± 2.1

[a] Mean of three experiments.
[b] CD content expressed as amount of cyclodextrin in NPs/total amount of CD used in NPs preparation × 100.

3.5. Mucoadhesive properties of Eudragit RS NPs

With the aim to gain information about the potential mucoadhesive properties of Eudragit RS 100 NPs, we evaluated the interaction between mucin and GSH-containing NPs without CD or NPs without GSH and CD by transmittance studies [28] employing polyacrylic acid, Carbopol 934 and PEG 6000 as control. According to this mucoadhesive test, the greater is the interaction between the NPs (or control) and mucin, the lower is the transmittance value of the tested sample due to the formation of macro-aggregates [28].

As shown in Fig. 3, the interaction after 15 h of incubation increased in the order PEG 6000 < polyacrylic acid << Carbopol 934 ~ GSH-containing NPs without CD and NPs without GSH and CD. Therefore, a conclusion of this study is that both GSH-containing NPs without CD and NPs without GSH and CD are able to interact efficiently with mucin and this can be explained simply by the interaction between Eudragit RS 100 and mucin due to their opposite charge, as already suggested for other Eudragit RS based NPs [29].

3.6. In vitro drug release studies

The suitability of the Eudragit RS 100 NPs for the release of GSH was studied *in vitro* at pH 1.2 and 6.8 which represent the approximate pH values of the stomach and intestinal membrane, respectively. Furthermore, we also decided to follow the release kinetics from NPs over a period of 6 h to limit GSH oxidation to GSSG which can occur especially in neutral-alkaline media [30]. Fig. 4 shows the cumulative percentages of GSH released at pH 1.2 (Panel a) and 6.8 (Panel b). It is apparent from the plots that the nature of the CD used significantly affected the amount of GSH released with greater amounts released at pH 6.8 compared to those at pH 1.2. Thus, at pH 6.8 about 80% of GSH was released from NPs containing γ-CD after 6 h while, under acidic conditions, all the NPs showed a release below the 50%. The corresponding release data after 6 h from NPs without any CD were about 23% and 15% at pH 1.2 and 6.8, respectively. At present, the reason(s) behind this different drug release behaviour at the two pH values considered is (are) not clear, since many factors are involved. These include different GSH loadings of the NPs studied, size of CD cavity, GSH/CD complex stability, influence of the CD on the T_{glass} of Eudragit RS 100, hydration of the matrix, drug solubility and diffusivity. A further important feature to be taken into account is that, as mentioned above, GSH is positively charged at pH 1.2, but negatively charged at pH greater than its pI (5.77) and consequently, on changing the pH of the medium, different electrostatic GSH-Eudragit RS 100- and/or hydrogen bonding GSH-CD-interactions occur leading to different drug release behaviours. Thus, to account for why NPs containing γ-CD showed the lowest release profile at pH 1.2 while the same NPs displayed the highest release profile at pH 6.8 it may be hypothesized that at pH 1.2 the hydrogen bonding interactions between the COOH groups of the GSH (positively charged, NH_3^+, COOH form) and the eight glucose units of γ-CD or Eudragit RS 100 might be strong bringing about a slow drug release. In contrast, in almost neutral conditions (pH 6.8) the hydrogen bonding interactions between the COO— groups of the GSH (negatively charged, NH_2, COO^- form) and γ-CD or Eudragit RS 100 might be lower leading to a prompt release. In the case of Me-β-CD the T_{glass} of the corresponding NPs is greater than that of pure Eudragit RS 100 (Fig. 2C) suggesting that a glassy matrix occurs with a lower drug diffusivity and it is irrespective of the pH release medium. From the data reported in Fig. 4 it is also evident that in most cases prolonged release profiles were observed as well as some systems generating different percentages of a burst effect were also noted (i.e., NPs containing γ-CD and HP-β-CD at pH 6.8). It seems that the amount of peptide in the outer shell and on the particle surface is released in the form of a burst, while the drug incorporated within the particle core is released over a more prolonged period. Finally, it should be noted that increasing amounts of GSSG were detected in neutral release medium, while at pH 1.2 no traces of disulfide were found by HPLC analysis.

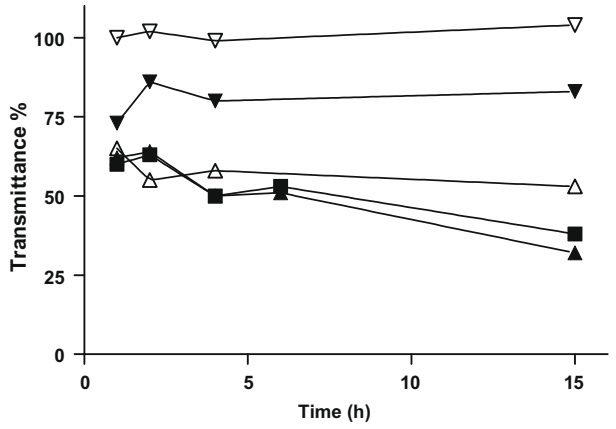

Fig. 3. Interaction studies between mucin and GSH-containing NPs without CD (■) or NPs without GSH and CD (▲) or polyacrylic acid (▼) or Carbopol 934 (Δ) or PEG 6000 (▽).

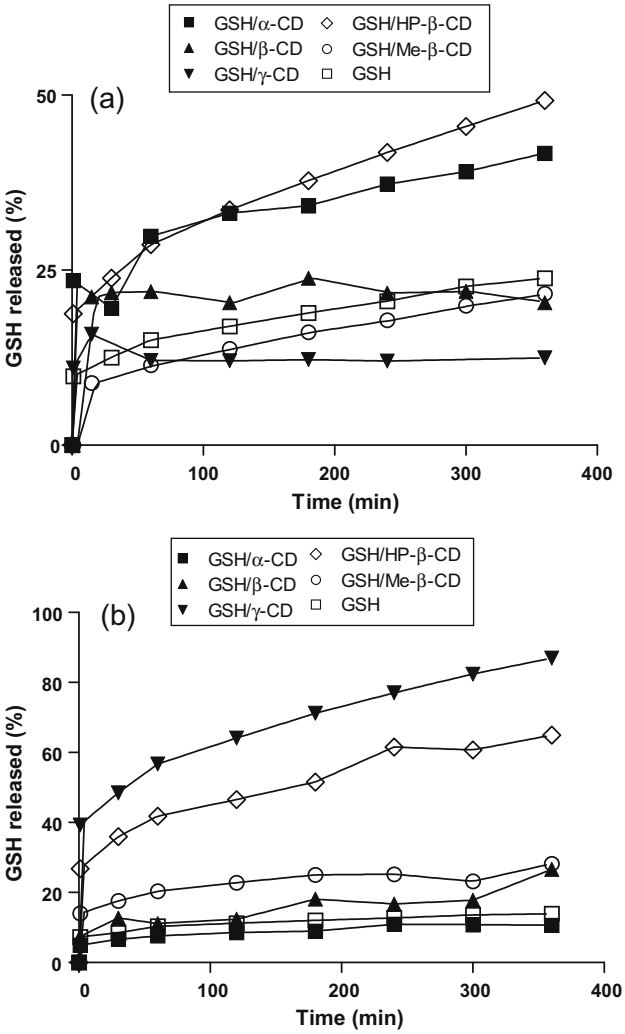

Fig. 4. GSH release kinetics at pH 1.2 (a) and pH 6.8 (b) ($n = 3$).

3.7. NP stability to enzymatic degradation

To evaluate NP stability to enzymatic degradation the representative system, GSH/Me-β-CD-loaded Eudragit RS 100 NPs as well as unencapsulated GSH were studied in the presence of γ-glutamyltranspeptidase. Under these conditions, free GSH showed a degradation with first-order kinetic ($t_{1/2}$ 76 min), while the corresponding first-order degradation of GSH/Me-β-CD-loaded Eudragit RS 100 NPs occurred with a $t_{1/2}$ of 107 min (Fig. 5).

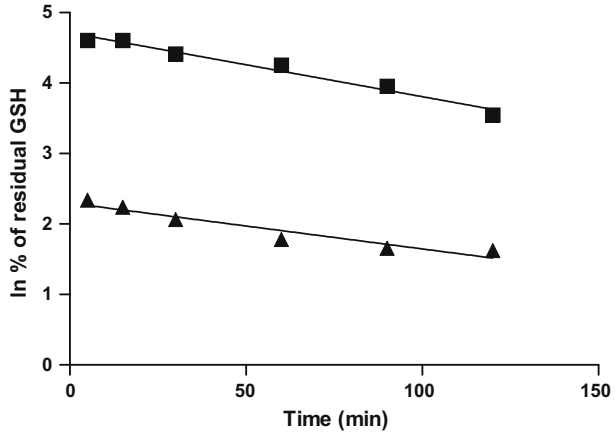

Fig. 5. Enzymatic degradation of the GSH/Me-β-CD-loaded Eudragit RS 100 NPs (▲) and unencapsulated GSH (■).

Therefore, from these data, it may be concluded that the encapsulation should prevent to some extent the enzymatic molecular degradation of the peptide.

3.8. Cytotoxicity of Eudragit RS 100 nanoparticles

A promising nanoparticle system intended for transmucosal administration of a peptide must be capable of delivering sufficient levels of the active agent without compromising the viability of the host cells. Published reports suggest that in general polycations are considered cytotoxic [31]. Eudragit RS 100, like most cationic macromolecules, could interact with anionic components (*N*-acetylneuraminic acid) of the glycoproteins on the surface of epithelial cells, causing cytotoxic effects. Therefore, the *in vitro* cytotoxicity studies of Eudragit RS 100 NPs with or without GSH and GSH/Me-β-CD were evaluated on human epithelial cells (HaCaT) and on murine monocyte macrophage cells (RAW 264.7) using the MTS assay. The choice of these cell lines was motivated by the following considerations: (i) HaCaT cell line grows as a stratified epithelium and can be thought to mimic the epithelial barrier to passive drug transport [32]; (ii) phagocytosis is the defence mechanism of the body and macrophages play an important role in host defence against infectious agents including pathogens, bacteria and viruses and moreover, NPs are susceptible to phagocytosis [33].

The viability of both cell lines HaCaT and RAW264.7 was determined after 48 and 72 h of NP treatment. Fig. 6 shows no detectable cytotoxicity after 48 and 72 h of incubation in both cell lines studied. Moreover, no significant difference in cellular growth was observed between the Eudragit RS 100, controls, and the GSH or GSH/Me-β-CD NPs. Overall, these outcomes suggest that the control, GSH- and GSH/Me-β-CD-loaded Eudragit RS 100 NPs may be considered as systems without cytotoxicity. Normal morphology was also observed by both light microscopy and TEM after 48 h of treatment with high doses of Eudragit RS 100 NPs with or without GSH (see Fig. 7).

The mitochondrial membrane potential ($\Delta\Psi$) was evaluated with the lipophilic cationic probe JC-1, which changes its colour reversibly from green to orange as $\Delta\Psi$ increases (over values of about 80–100 mV). This is due to the reversible formation of JC-1 aggregates upon membrane polarization causing shifts in light emission from 530 nm (emission of JC-1 in monomeric form) to 590 nm (emission of JC-1 aggregates). Treated cells with GSH-Eudragit RS 100 NPs (Fig. 8B) and Eudragit RS 100 NPs (Fig. 8C)

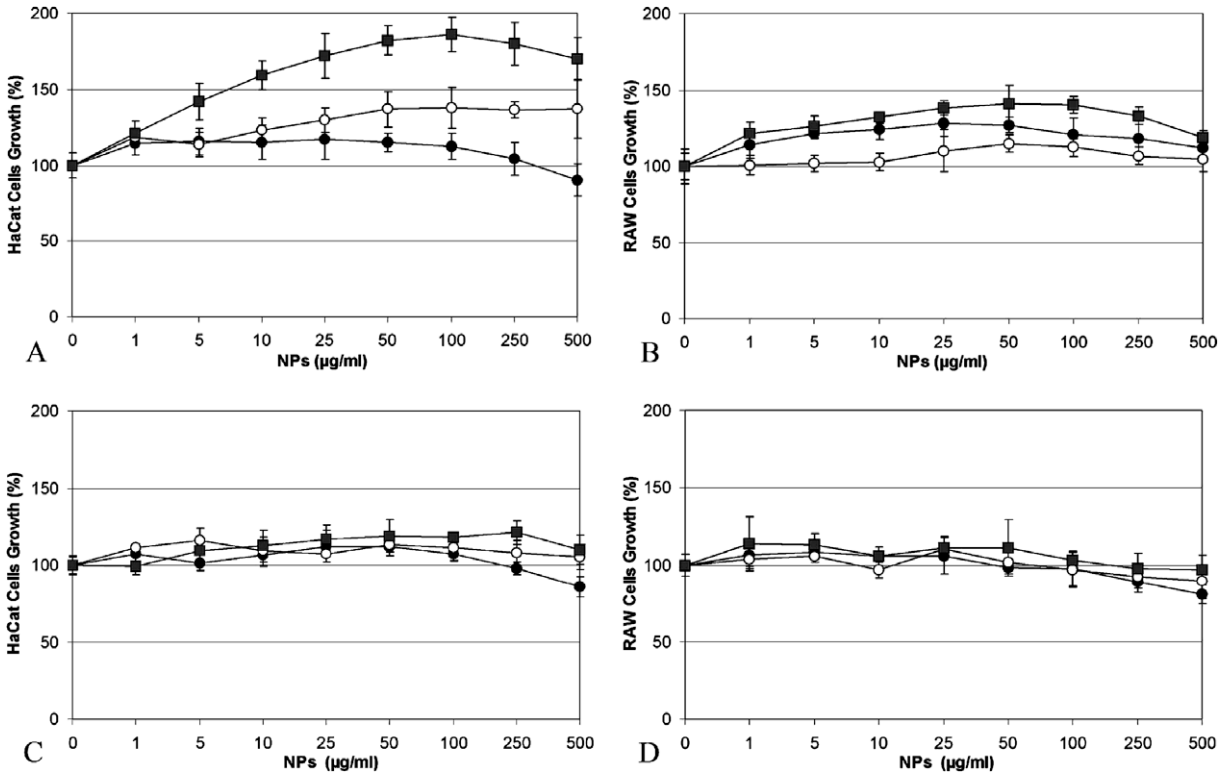

Fig. 6. Cytotoxicity on HaCaT cell line (A and C) and RAW 264.7 (B and D). Cellular viability was evaluated using the MTS assay as described under Section 2 with increasing percentages (0–500 µg/ml) of NPs. Control Eudragit RS 100 NPs (empty circles), GSH Eudragit RS 100 NPs (filled circles) and GSH/Me-β-CD-loaded Eudragit RS 100 NPs. The growth was measured at 48 h (A and B) and 72 h (C and D). The values represent the percentage calculated with respect to untreated cells. Each data point represents the mean ± SD of octuplicate samples from two different experiments.

at 250 μg/ml for 48 h show a similar distribution of JC-1 with respect to the control cells (Fig. 8A). The mitochondrial functionality of HaCaT cells was also not affected by treatment with high doses of Eudragit RS 100 NPs with or without GSH. Similar results were also obtained on 264.7 cell line (data not shown).

3.9. Transport studies in frog intestine

Another important factor to be taken into account for the transmucosal delivery of therapeutic peptides is the presence of the apical mucus layer on the epithelium surface since it may influence the absorption of compounds. Recently, we have found that the frog intestine is a reliable model for assessing intestinal permeability [34,35] and it is known that an apical mucus layer is present in this intestine. Distinct advantages of this new screening tool for assessing intestinal permeability are a relatively easy isolation of frog intestine, no need to be exposed to O_2/CO_2 atmosphere and lower feeding requirements as compared with conventional animal models (typically rodents) that requires thermostatation and glucose as a nutrient. Therefore, in order to predict the *in vivo* behaviour of GSH/CD NPs after oral administration, transport experiments through frog intestine were carried out.

It should be noted that in preliminary experiments using GSH- and GSH/Me-β-CD-loaded NPs, peptide transport was not observed. This may be related to the low GSH loading of the NPs studied and to the fact that the frog intestine is less permeable

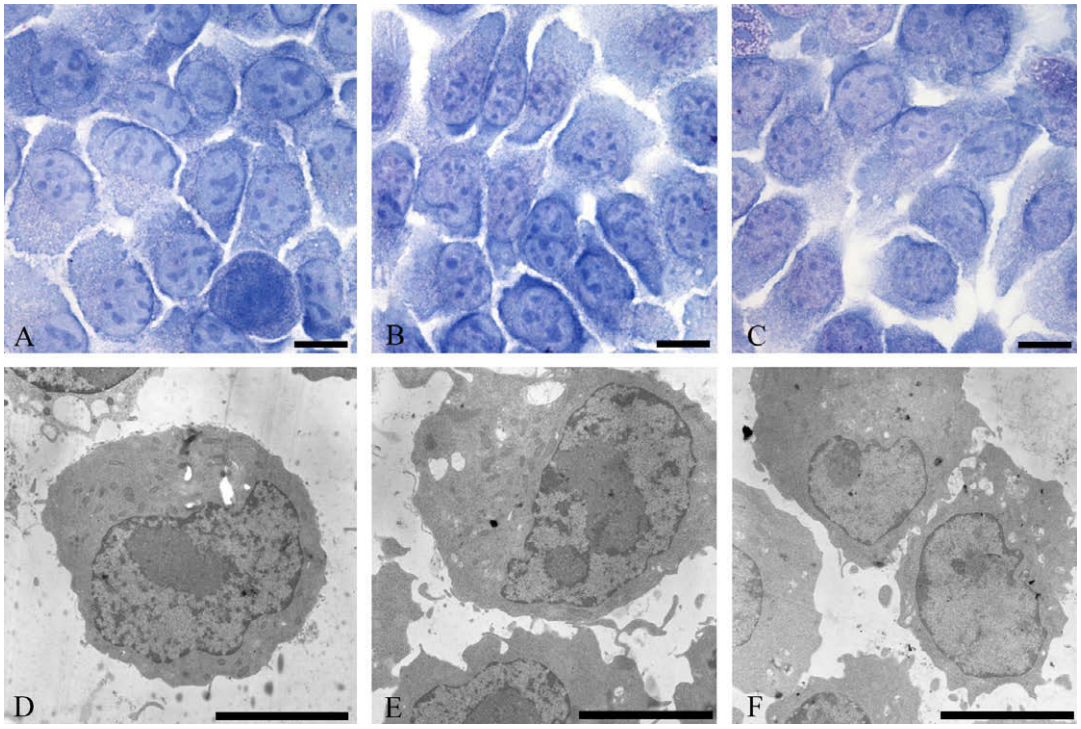

Fig. 7. Light and electron microscopy performed on human keratinocyte cell line (HaCaT). Cells were untreated (control) (A and D) or treated with Eudragit RS 100 NPs (B and F) or with GSH-Eudragit RS 100 NPs (C and F) at 250 μg/ml for 48 h. (Bars 5 μm).

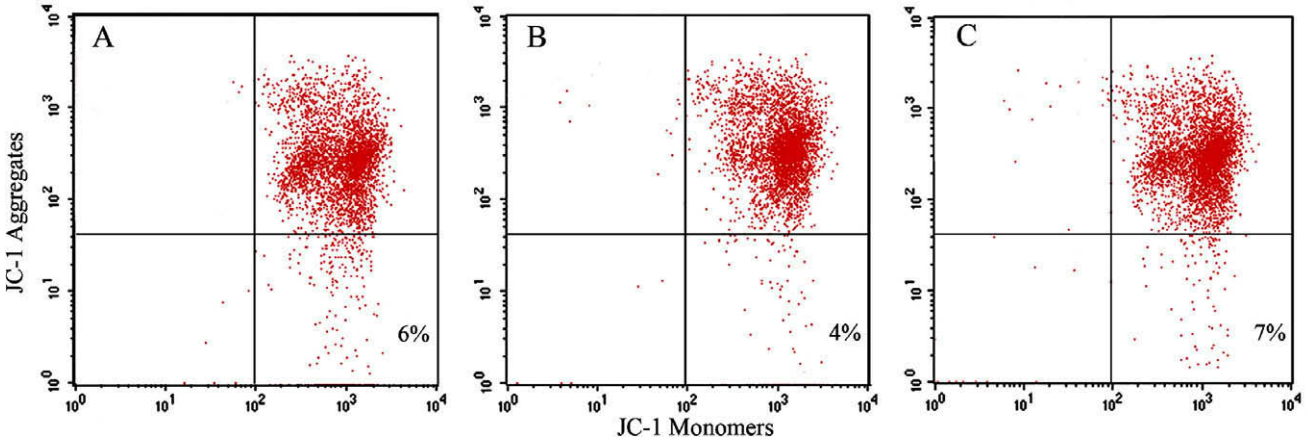

Fig. 8. Representative examples of fluorescence pattern of cells stained with JC-1. Distribution of JC-1: both monomeric and aggregated forms appear in control (A) and cells treated with GSH- Eudragit RS 100 NPs (B) and Eudragit RS 100 NPs (C) at 250 μg/ml for 48 h, suggesting an identical $\Delta\Psi$. Numbers indicate the percentage of cells with depolarized mitochondria.

than the human one [34,35]. Taking into account that mucoadhesive and positively charged polymers may cause a transient opening of the epithelial tight junctions [36] thus enhancing the permeation of hydrophilic substances, the co-administration of the peptide and control- or Me-β-CD-loaded Eudragit RS 100 NPs was evaluated. Based on the cumulative amount of GSH transported after 6 h, the order of apparent permeability coefficients (Papp) was Me-β-CD-loaded Eudragit RS 100 NPs (3.95×10^{-6} cm/s) > control (3.81×10^{-6} cm/s) > peptide alone (3.70×10^{-6} cm/s). Although there were no statistically significant differences in Papp values, the observed trend might lend support to the hypothesis of an enhancement role played by NPs and particularly of CD-containing NPs. However, further study is necessary to draw more definitive conclusions in this regard.

4. Conclusions

The present study reports the preparation and physicochemical characterization of nanoparticles which combine the mucoadhesive properties of Eudragit RS 100 with the penetration enhancing properties of CDs. The results indicate that both the mean diameter and the surface charge on NPs were not markedly affected by the presence of CDs. It has been shown that the presence of the oligosaccharide influences drug release and, to some extent, peptide stability whereas no or negligible effect was noted on drug loading. Moreover, data suggest that electrostatic interactions should not be relevant for the entrapment of GSH within the NPs. In comparison with CD/Eudragit RS 100 microparticles previously reported [20,21], the corresponding nanocarriers herein studied suffer from a peptide loading point of view (i.e., 57–81% vs 15–24%, respectively). However, the capability of Eudragit RS 100 NPs to interact efficiently with mucin and deliver GSH along transmucosal routes could provide peculiar features to these formulations, despite their relatively low E.E. Finally, it has been shown that CD/Eudragit RS 100 NPs may be used for transmucosal absorption of GSH. CD/Eudragit RS 100 NPs did not alter cellular proliferation of the two cell lines (HaCaT and RAW264.7) nor the mitochondrial functionality or the cellular morphology of HaCaT cells. Due to the lack of cytotoxity in the HaCaT cell line, we believe that these formulations could be also used for dermal delivery of GSH. It is also well known that UV-A and UV-B irradiation can cause damage through an excess of reactive oxygen species (ROS) produced by human keratinocytes [37] leading to intracellular GSH depletion involved in the pathogenesis of several cutaneous disorders [38]. In this regard, further studies are in progress and the results will be reported in due course.

Acknowledgments

Thanks are due to Roquette Italia (Cassano Spinola, Italy) and Waker Chemie (Peschiera Borromeo, Italy) for the kind gifts of CDs. A.T. acknowledge the Electronic Microscopy Service staff of the Department of Pharmaceutical Technology, University of Santiago de Compostela, Spain, for TEM analyses. The authors express their thanks to Dr. Laviano (Dipartimento Geomineralogico dell'Università di Bari) for his help in recording X-ray spectra. This work was supported by a grant from Ministero dell'Istruzione, dell'Università e della Ricerca (MIUR) e fondi di Ateneo.

References

[1] A.K. Banga, Therapeutic Peptides and Proteins: Formulation, Processing, and Delivery Systems, second ed., CRC Press Taylor and Francis, London, UK, 2006.
[2] A.T. Florence, D. Attwood, Physicochemical Principles of Pharmacy, fourth ed., Pharmaceutical Press, London, UK, 2006, pp. 431–461.
[3] C. Prego, M. Garcia, D. Torres, M.J. Alonso, Transmucosal macromolecular drug delivery, J. Control. Release 101 (2005) 151–162.
[4] N. Csaba, M. Garcia-Fuentes, M.J. Alonso, The performance of nanocarriers for transmucosal drug delivery, Expert Opin. Drug Deliv. 3 (2006) 463–478.
[5] E. Alleman, J.C. Leroux, R. Gurny, Polymeric nano- and micro-particles for the oral delivery of peptides and peptidomimetics, Adv. Drug Deliv. Rev. 34 (1998) 171–189.
[6] P. Jenner, Oxidative stress in Parkinson's disease and other neurodegenerative disorders, Pathol. Biol. 44 (1996) 57–64.
[7] A.M. Samuni, E.Y. Chuang, M.C. Krishna, W. Stein, W. DeGraff, A. Russo, J.B. Mitchell, Semiquinone radical intermediate in catecholic estrogen-mediated cytotoxicity and mutagenesis: Chemoprevention strategies with antioxidants, Proc. Natl. Acad. Sci. USA 100 (2003) 5390–5395.
[8] E.W. Flagg, R.J. Coates, D.P. Jones, T.E. Byers, R.S. Greenberg, G. Gridley, J.K. McLaughlin, W.J. Blot, M. Haber, S. Preston-Martin, Dietary glutathione intake and the risk of oral and pharyngeal cancer, Am. J. Epidemiol. 139 (1994) 453–465.
[9] S. Mihm, J. Ennen, U. Pessara, V. Kurth, W. Droge, Inhibition of HIV-1 replication and NF-kappa B activity by cysteine and cysteine derivatives, AIDS 5 (1991) 497–503.
[10] L. Carter-Dawsona, F. Shen, R.S. Harwerth, M.L.J. Crawford, E.L. Smith, A. Whitetree, Glutathione content is altered in Müller cells of monkey eyes with experimental glaucoma, Neurosci. Lett. 364 (2004) 7–10.
[11] N. Langoth, A. Bernkop-Schnurch, P. Kurka, The inhibitory effect of glutathione on buccal enzymatic degradation of therapeutic peptides (leu-enkephalin, luteinizing hormone-releasing hormone and pituitary adenylate cyclase activating peptide), J. Drug Del. Sci. Tech. 15 (2005) 435–438.
[12] R. Pignatello, C. Bucolo, P. Ferrara, A. Maltese, A. Puleo, G. Puglisi, Eudragit RS 100 nanosuspension for the ophthalmic controlled delivery of ibuprofen, Eur. J. Pharm. Sci. 16 (2002) 53–61.
[13] N. Ubrich, C. Schmidt, R. Bodmeier, M. Hoffman, P. Maincent, Oral evaluation in rabbits of cyclosporine-loaded Eudragit RS or RL nanoparticles, Int. J. Pharm. 288 (2005) 69–175.
[14] C. Vaquette, V.G. Babak, F. Baros, O. Boulanouar, D. Dumas, P. Fievet, N.R. Kildeeva, P. Maincent, X. Wang, Zeta-potential and morphology of electrospun nano- and microfibers from biopolymers and their blends used as scaffolds in tissue engineering, Mendeleev Commun. 18 (2008) 38–41.
[15] H. Boudad, P. Legrand, G. Lebas, M. Cheron, D. Duchêne, G. Ponchel, Combined hydroxypropyl-beta-cyclodextrin and poly(alkylcyanoacrylate) nanoparticles intended for oral administration of saquinavir, Int. J. Pharm. 218 (2001) 113–124.
[16] B. Haeberlin, T. Gengenbacher, A. Meinzer, G. Fricker, Cyclodextrins-useful excipients for oral peptide administration? Int. J. Pharm. 137 (1996) 103–110.
[17] T. Irie, K. Uekama, Cyclodextrins in peptide and protein delivery, Adv. Drug Deliv. Rev. 36 (1999) 101–123.
[18] K. Kafedjiiski, M. Werle, F. Foger, A. Bernkop-Schnürch, Synthesis and in vitro characterization of a novel poly(acrylic acid)-glutathione conjugate, J. Drug Del. Sci. Tech. 15 (2005) 411–417.
[19] D.M. Townsend, K.D. Tew, H. Tapiero, The importance of glutathione in human disease, Biomed. Pharmacother. 57 (2003) 145–155.
[20] A. Trapani, V. Laquintana, N. Denora, A. Lopedota, A. Cutrignelli, M. Franco, G. Trapani, G. Liso, Eudragit RS 100 microparticles containing 2-hydroxypropyl-beta-cyclodextrin and glutathione: physicochemical characterization, drug release and transport studies, Eur. J. Pharm. Sci. 30 (2007) 64–74.
[21] A. Lopedota, A. Trapani, A. Cutrignelli, V. Laquintana, N. Denora, M. Franco, G. Trapani, G. Liso, Effect of cyclodextrins on physico-chemical and release properties of Eudragit RS 100 microparticles containing glutathione, J. Incl. Phenom. Macrocycl. Chem. 57 (2007) 425–432.
[22] L. Gate, C. Vauthier, P. Couvreur, K.D. Tew, H. Tapiero, Glutathione-loaded poly(isobutylcyanoacrylate) nanoparticles and liposomes: comparative effects in murine erythroleukemia and macrophage-like cells, S.T.P. Pharma Sci. 11 (2001) 355–361.
[23] Y. Kawashima, T. Niwa, T. Handa, H. Takeuchi, T. Iwamoto, K. Itho, Preparation of controlled-release microspheres of ibuprofen with acrylic polymer by a novel quasi-emulsion solvent diffusion method, J. Pharm. Sci. 78 (1989) 68–72.
[24] S. Galindo-Rodriguez, E. Allemann, H. Fessi, E. Doelker, Physicochemical parameters associated with nanoparticle formation in the salting-out, emulsification-diffusion, and nanoprecipitation methods, Pharm. Res. 21 (2004) 1428–1439.
[25] A.M. Da Silveira, G. Ponchel, F. Puisieux, D. Duchene, Combined poly(isobutylcyanoacrylate) and cyclodextrins nanoparticles for enhancing the encapsulation of lipophilic drugs, Pharm. Res. 15 (1998) 1051–1055.
[26] M. Garcia-Fuentes, A. Trapani, M.J. Alonso, Protection of the peptide glutathione by complex formation with alpha-cyclodextrin: NMR spectroscopic analysis and stability study, Eur. J. Pharm. Biopharm. 64 (2006) 146–153.
[27] C. Donini, D.N. Robinson, P. Colombo, F. Giordano, N.A. Peppas, Preparation of poly(methacrylic acid-g-poly(ethylene glycol)) nanospheres from methacrylic monomers for pharmaceutical applications, Int. J. Pharm. 245 (2002) 83–91.
[28] S. Rossi, F. Ferrari, M.C. Bonferoni, C. Caramella, Characterization of chitosan hydrochloride–mucin interaction by means of viscosimetric and turbidimetric measurements, Eur. J. Pharm. Sci. 10 (2000) 251–257.
[29] A. Lamprecht, P. Koenig, N. Ulbrich, P. Maincent, D. Neumann, Low molecular weight heparin nanoparticles: mucoadhesion and behavior in Caco-2 cells, Nanotechnology 17 (2006) 3673–3680.
[30] E. Camera, M. Picardo, Analytical methods to investigate glutathione and related compounds in biological and pathological processes, J. Chromatogr. B 781 (2002) 81–206.

[31] D.M. Morgan, V.L. Larvin, J.L. Pearson, Biochemical characterization of polycation-induced cytotoxicity to human vascular endothelial cells, J. Cell. Sci. 94 (1989) 553–559.
[32] N. Maas-Szabowski, A. Starker, N.E. Fusenig, Epidermal tissue regeneration and stromal interaction in HaCaT cells is initiated by TGF-α, J. Cell. Sci. 116 (2003) 2937–2948.
[33] F. Ahsan, I.P. Rivas, M.A. Khan, A.I. Torres Suarez, Targeting to macrophages: role of physicochemical properties of particulate carriers – liposomes and microspheres – on the phagocytosis by macrophages, J. Control. Release 79 (2002) 29–40.
[34] G. Trapani, M. Franco, A. Trapani, A. Lopedota, A. Latrofa, E. Gallucci, S. Micelli, G. Liso, Frog intestinal sac: a new *in vitro* method for the assessment of intestinal permeability, J. Pharm. Sci. 93 (2004) 2909–2919.
[35] M. Franco, A. Lopedota, A. Trapani, A. Cutrignelli, D. Meleleo, S. Micelli, G. Trapani, Frog intestinal sac as an *in vitro* method for the assessment of intestinal permeability in humans: application to carrier transported drugs, Int. J. Pharm. 352 (2008) 182–188.
[36] N.G. Shipper, S. Olsson, J.A. Hoogstrate, A.G. deBoer, K.M. Varum, P. Artusson, Chitosans as absorption enhancers for poorly absorbable drugs: 2. Mechanism of absorption enhancement, Pharm. Res. 14 (1997) 923–929.
[37] A. Svobodová, A. Zdarilová, D. Walterová, J. Vostálová, Flavonolignans from Silybum marianum moderate UVA-induced oxidative damage to HaCaT keratinocytes, J. Dermatol. Sci. 48 (2007) 213–224.
[38] M. Zhu, G.T. Bowden, Molecular mechanism(s) for UV-B irradiation-induced glutathione depletion in cultured human keratinocytes, Photochem. Photobiol. 80 (2004) 191–196.